

Fractal properties and critical exponents in tumor*

Miguel Martín-Landrove^{1,2**} y Demián Pereira^{1,3}

¹Centro de Resonancia Magnética, Escuela de Física, Facultad de Ciencias.

²Posgrado de Física Médica, Facultad de Ciencias. ³Laboratorio de Ensayos no Destructivos, Facultad de Ingeniería. Universidad Central de Venezuela, Apartado 47586, Caracas 1041A, Venezuela.

Recibido: 30-11-05 Aceptado: 10-04-06

Abstract

In general, tumors exhibit irregular borders with geometrical properties which are expected to depend upon their degree of malignancy. To appropriately evaluate these irregularities, it is necessary to apply segmentation procedures on the image that clearly define the active region of the tumor and its border. In the present work, nosologic maps were obtained combining T_2 -weighted magnetic resonance images with *in vivo* magnetic resonance spectroscopy information on brain tumors. The image was segmented according to the nosologic map and tumor contours were determined. Several fractal properties were determined on the contour: the capacity or fractal dimension, the correlation dimension for a temporal series constructed from the original contour, and also a critical exponent coming from the contour roughness. The results obtained showed a good correlation between the roughness critical exponent and the degree of malignancy of the tumor.

Key words: critical exponents, fractal dimension, segmentation, tumor, nosologic map.

Propiedades fractales y exponentes críticos en tumores

Resumen

Los tumores presentan por lo general una frontera irregular cuyas propiedades geométricas pueden variar según el grado de malignidad. Para evaluar de forma apropiada esta irregularidad se hace necesario aplicar metodologías de segmentación de imágenes que permitan definir precisamente la región activa del tumor y, así, claramente su frontera. En el presente trabajo se obtuvieron mapas nosológicos combinando imágenes de resonancia magnética ponderadas en T_2 con información de espectroscopias *in vivo* por resonancia magnética sobre tumores de cerebro. La imagen fue segmentada de acuerdo al mapa nosológico y se determinaron los contornos del tumor. Varias propiedades fractales se determinaron sobre el contorno: la dimensión fractal o de capacidad, la dimensión de correlación para una serie temporal construida a partir del contorno y también un exponente crítico proveniente de la rugosidad del contorno. Los resultados obtenidos demuestran una buena correlación entre el exponente crítico asociado a la rugosidad del contorno y el grado de malignidad del tumor.

Palabras claves: exponentes críticos, dimensión fractal, segmentación, tumor, mapa nosológico.

* Trabajo presentado en el V Congreso de la Sociedad Venezolana de Física, Universidad del Zulia. Nucleo Punto Fijo - Edo. Falcón, Venezuela, Noviembre 2005.

** Autor para la correspondencia. E-mail: mmartin@fisica.ciens.ucv.ve

Introduction

Tumor growth is a complex process ultimately dependent on tumor cells proliferating and spreading in host tissues. As with many natural colonies, cell colonies are fractal (1-3) and the description of their complex contours using classical Euclidean geometry is very difficult to provide. However, the fractal nature of the contours allows for scaling analysis to characterize their dynamic behavior and therefore can be used to determine tumor growth or progression. Recent studies of *in vitro* tumor cell colonies and resected tumor sections (4, 5) demonstrate that some kind of universality in tumor growth dynamics can be determined through the evaluation of fractal properties and critical exponents. The purpose of this work is to obtain fractal parameters and critical exponents of contours in tumor sections obtained by MRI in order to determine a possible correlation between tumor grade or stage and these parameters. The problem involves the segmentation of the tumor image, which is a difficult task compared with determinations performed on resected tumor sections where the histopathological analysis is always possible. The segmentation of brain tumor images can be accomplished by *in vivo* MR spectroscopy determinations to obtain nosologic images or maps (6), i.e., mapping of the pathology or tissue type, and more recently by image fusion with other MR modalities (7).

Materials and methods

Brain tumor images were obtained by MR T_2 -weighted multiecho technique on a Siemens Magnetom scanner working at a magnetic field of 1.5 T. *In vivo* MR spectroscopy information was combined with these images to obtain nosologic maps for the spatial extension of the disease according to reference (7). The contours obtained from the segmentation of the nosologic maps were analyzed to determine the capacity or Hausdorff dimension by a box counting procedure:

$$D_0 = -\lim_{\varepsilon \rightarrow 0} \frac{\ln N(\varepsilon)}{\ln(\varepsilon)} \quad [1]$$

where $N(\varepsilon)$ is the number of boxes of size ε that include points in the contour. Time series were constructed as follows: the "center" of the contour is determined and for each point, its radius from this "center" was calculated, giving an entry for the time series. These series will be called radial time series. The correlation dimension for each time series generated was determined by the Grassberger-Procaccia method (8, 9), with:

$$D_2 = \lim_{\varepsilon \rightarrow 0} \frac{\ln C_2(\varepsilon)}{\ln \varepsilon} \quad [2]$$

and:

$$C_2(\varepsilon) \approx \lim_{N \rightarrow \infty} \frac{1}{N(N-1)} \sum_{i=1}^N \sum_{j=1, j \neq i}^N \Theta(\varepsilon - |x_i, x_j|) \quad [3]$$

where N is the number of points in the time series and Θ is the Heaviside step function. To estimate the critical exponents given by references (4, 5) data coming from the time series could be used and so, the mean radius of tumor contour is:

$$\langle r \rangle = \frac{1}{N} \sum_{i=1}^N r_i(t) \quad [4]$$

and the contour roughness is defined as:

$$w(l, t) = \left\{ \frac{1}{l} \sum_{r_i \in l} [r_i(t) - \langle r \rangle_l]^2 \right\}_L^{1/2} \quad [5]$$

where L is the total length of the contour, $\langle \rangle_l$ is the average over a length l , $\{ \}_L$ is the average over L and t is the time. Figure 1 shows how these variables are selected in this work. Equation 2 exhibits the scaling property with l :

$$w(l, t) = l^{\alpha_{loc}} \quad [6]$$

where α_{loc} is a roughness critical exponent. Tumor data, either coming from resected sections or from images, exhibit a time evo-

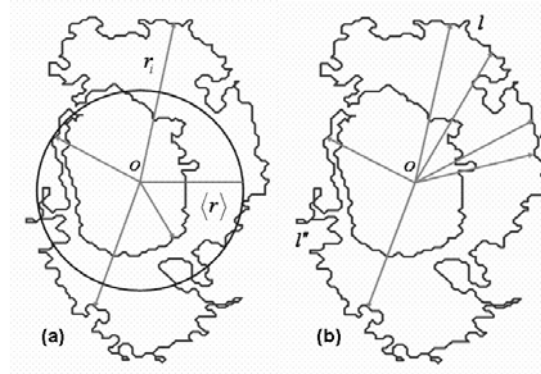


Figure 1. (a) Typical geometry for the estimation of the mean radius of the tumor. (b) Several lengths l for the estimation of the averages defined in the text.

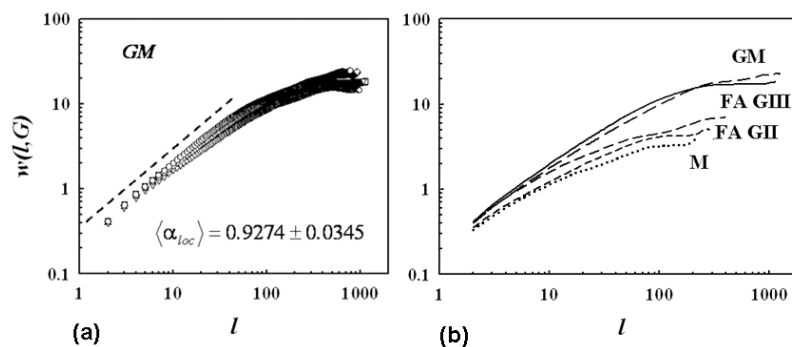


Figure 2. (a) Scaling property in a glioblastoma multiforme (Grade IV). (b) Scaling property for different tumors: GM, glioblastoma multiforme, FA, fibrillar astrocytoma, Grades II and III, and M, meningioma, a low grade tumor.

lution that can not be accurately estimated and typically a fuzzy variable is used, i.e., tumor grade. It is assumed that similar tumor grade corresponds to also similar dynamical state and therefore to a particular value α^{loc} .

Results and discussion

The scaling property of the contour roughness is shown in figure 2a for axial images of a glioblastoma multiforme. Similar results are obtained for tumors with different grade as shown in figure 2b, where it can be seen that different tumor grades exhibit different values of α^{loc} , within the range between 0.7923 and 0.9274. In figure 3, it is shown

the evaluation of the capacity dimension for a glioblastoma multiforme using the box counting method. The different curves come from different axial images taken at different levels across the tumor. Notice that there is a saturation effect that comes from the limit in the minimum scale imposed by the pixel size (that also limits the number of points in the contour). For the tumors analyzed, capacity dimension yielded values within the range from 1.1206 to 1.2663. Examples of time series that can be obtained from the contour are shown in figure 4. On the left of the figure, it is represented the radial time series used to calculate the correlation dimension in this work, previously defined, and on the right, a time series that can be obtained by

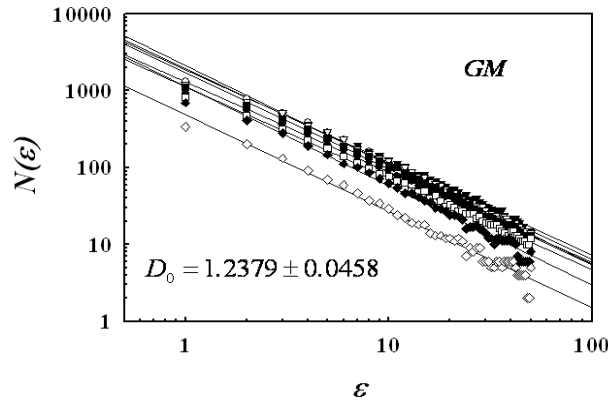


Figure 3. Box counting procedure to determine Hausdorff dimension in a glioblastoma multiforme. Each curve comes from the analysis in a contour corresponding to a different image slice. The variation in the slope comes from the limit in the smallest scale, i.e., pixel size.

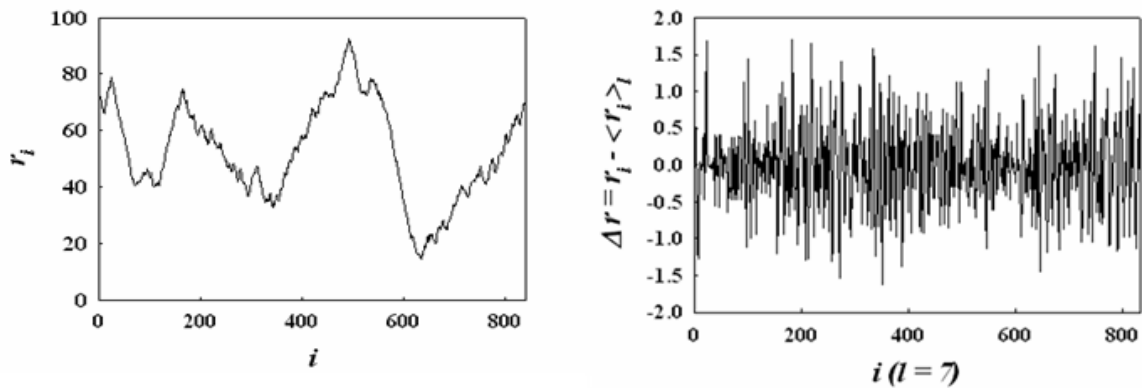


Figure 4. Time series obtained from the contour points. On the left, the time series for the radius of the contour point, as described in the text and on the right, the time series as a difference with respect to a moving average.

taking differences with respect to a moving average, somewhat reflecting the roughness property of the contour. Series of this type will be analyzed in future work. Finally in Figure 5, correlations of the fractal parameters and roughness critical exponent with tumor grade are shown.

Conclusions

It has been demonstrated that tumors exhibit fractal properties that can be de-

termined through the analysis of medical images. The roughness critical exponent agree well with other results (4, 5) and showed a significant correlation with tumor grade that deserves further analysis and statistics to establish a correlation with dynamical tumor growth models. Future work will be aimed to the analysis of time series related to contour roughness in 2D and 3D image data sets.

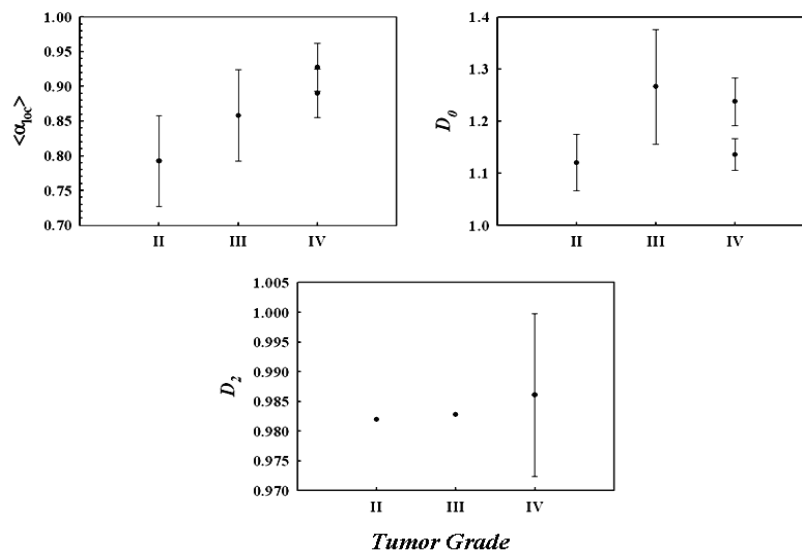


Figure 5. Correlations between the calculated parameters: α_{loc} , D_0 and D_2 with the tumor grade. For the analysis, tumors that are related histologically were only considered.

References

1. LOSA G.A., BAUMANN G., NONNENMACHER T.F. *Pathol. Res. Pract.* 188: 680-686, 1992.
2. CROSS S.S., MCDONAGH A.J.C., STEPHENSON T.J., COTTON D.W., UNDERWOOD J.C. *Am. J. Dermatopathol* 17: 374-378, 1995.
3. LOSA G.A. *Pathologica* 87: 310-317, 1995.
4. BRÚ A., PASTOR J.M., FERNAND I., MELLE S., BRÚ I. *Phys. Rev. Lett.* 81: 4008-4011, 1998.
5. BRÚ A., ALBERTOS S., SUBIZA J.L., LÓPEZ GARCÍA-ASENJO J., BRÚ I., *Biophys. J.* 85: 2948-2961, 2003.
6. SZABO DE EDELENYI F., RUBIN C., ESTÈVE F., GRAND S., DÉCORPS M., LEFOURNIER V., LE-BAS J.-F., RÉMY C. *Nature Medicine* 6: 1287-1289, 2000.
7. MARTÍN-LANDROVE M., BAUTISTA I., MAYOBRE F., VILLALTA R., CONTRERAS A. *Magma* 15: 23-24, 2002.
8. GRASSBERGER P., PROCACCIA I. *Phys. Rev. Lett.* 50: 346-349, 1983.
9. SPROTT J.C., ROWLANDS G. *International Journal of Bifurcation and Chaos* 11: 1865-1880, 2001.